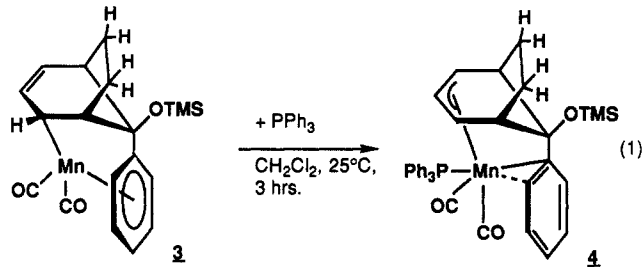


**Figure 1.** Molecular structure and labeling scheme for **4**. Distances (Å): Mn–P, 2.266 (3); Mn–C(5), 2.265 (11); Mn–C(6), 2.081 (11); Mn–C(7), 2.214 (11); Mn–C(11), 2.445 (10); Mn–C(12), 2.567 (10). Angles (deg): C(1)–Mn–C(2), 105.5 (5); C(1)–Mn–P, 85.5 (4); C(2)–Mn–P, 83.8 (4); P–Mn–C(11), 167.3 (3); C(1)–Mn–C(11), 104.4 (5); C(2)–Mn–C(11), 85.9 (4); C(5)–C(6)–C(7), 118.2 (9).

Complex **3** is an unusual analogue of other arene-alkyl manganese complexes prepared by both the Brookhart<sup>8</sup> and Sweigart<sup>9</sup> groups, in which the former showed that alkyl migration to the endo face of the arene could be induced by addition of PPh<sub>3</sub>.<sup>8</sup> We have therefore reacted **3** with PPh<sub>3</sub> in an attempt to promote coupling of the metal  $\sigma$ -bonded carbon C(4) and the phenyl substituent. However, a more unusual reaction forming a highly distorted  $\eta^2$ -arene complex occurred. Thus, addition of 1–2 equiv of PPh<sub>3</sub> to **3** in CH<sub>2</sub>Cl<sub>2</sub> results in the formation of **4** containing an ( $\eta^3$ -allyl)Mn(CO)<sub>2</sub>(PPh<sub>3</sub>) fragment  $\eta^2$ -bonded to the phenyl ring, eq 1.



Complex **4** was isolated in 40% yield (based on **3**) as analytically pure deep red microcrystals. Its structure was confirmed by <sup>1</sup>H, <sup>13</sup>C, and <sup>31</sup>P NMR and IR spectroscopy,<sup>6</sup> as well as by an X-ray diffraction study.<sup>10</sup> An ORTEP drawing of **4** is shown in Figure 1 and shows a pseudooctahedral structure about manganese with the phosphine and  $\eta^2$ -phenyl ligand trans to one another. The Mn–C(11) distance of 2.445 (10) Å is clearly a bond, albeit weak, and the long Mn–C(12) distance of 2.567 (10) Å suggests that both C(11) and C(12) are involved in a highly distorted  $\eta^2$ -arene-metal interaction. The Mn...C(16) distance is 3.250 (11) Å. The distortion in the  $\eta^2$ -ligand is such that it appears almost  $\eta^1$ -bonded to manganese; however, a twist of the phenyl ring about the C(3)–C(11) axis and a tilt of the bicyclic ligand brings C(12) close to the metal.<sup>11</sup>

(8) (a) Brookhart, M.; Pinhas, A. R.; Lukacs, A. *Organometallics* **1982**, 1, 1730. (b) Rush, P. K.; Noh, S. K.; Brookhart, M. *Organometallics* **1986**, 5, 1745.

(9) Halpin, W. A.; Williams, J. C., Jr.; Hanna, T.; Sweigart, D. A. *J. Am. Chem. Soc.* **1989**, 111, 376.

(10) Crystal data for **4**: C<sub>37</sub>H<sub>38</sub>MnO<sub>2</sub>PSi, monoclinic, *P*2<sub>1</sub>/c, *a* = 10.153 (4) Å, *b* = 9.741 (3) Å, *c* = 33.346 (11) Å,  $\beta$  = 96.24 (3)°, *V* = 3278.5 (24) Å<sup>3</sup>, *Z* = 4, *D* (calcd) = 1.306 g cm<sup>−3</sup>,  $\mu$  (Mo K $\alpha$ ) = 5.03 cm<sup>−1</sup>, *T* = 293 K. Of 3769 data collected (Nicolet R3m diffractometer, 4° ≤ 2 $\theta$  ≤ 42° with no higher angle data omitted), 3424 were independent and 1989 with *F*<sub>o</sub> ≥ 5 $\sigma$ (*F*<sub>o</sub>) were observed. Solution was by direct methods, and refinement included anisotropic thermal parameters for all non-hydrogen atoms. Hydrogen atoms were idealized, and the phenyl rings in PPh<sub>3</sub> were constrained to rigid hexagons. *R*<sub>F</sub> = 8.08%, *R*<sub>wF</sub> = 8.08%, *S* = 1.976, and  $\Delta\rho$  = 1.58 e/Å<sup>3</sup>. Computations used SHELXTL software.

(11) A referee has noted that this tilt results in an asymmetry in the  $\eta^3$ -allyl bonding such that C(7) is 0.051 Å closer to Mn than C(5).

Complex **4** is stable as a solid, but in solution, a small amount of **3** and free PPh<sub>3</sub> are also observed, indicating a delicate balance between  $\eta^2$ - and  $\eta^6$ -arene ligation. Noteworthy is that the NMR data for **4** suggest no arene bonding to Mn (e.g., no <sup>31</sup>P coupling to the arene carbons and only four arene <sup>13</sup>C NMR resonances), which may be due to a rapid complexation/decomplexation of the arene double bond in solution. Surprisingly, addition of excess PPh<sub>3</sub> to **3** does not form a Mn(CO)<sub>2</sub>(PPh<sub>3</sub>)<sub>2</sub> derivative with complete arene dissociation, presumably due to steric factors, and may explain the stability of the novel structure **4**.

The formation of **3** demonstrates a potentially viable approach to the construction of bicyclic ring systems via the intramolecular coupling of two unsaturated ligands at a metal center. In addition, the reaction of **3** with PPh<sub>3</sub> indicates that facile decomplexation of the organic moiety should be possible via treatment with added ligands followed by protonation of the remaining M–C  $\sigma$ -bond. Further studies on **3** and **4** involving the functionalization of the bicyclo[3.2.1]oct-2-ene ring and other diene-yl-carbene complexes are in progress.

**Acknowledgment.** We are grateful to the donors of the Petroleum Research Fund, administered by the American Chemical Society, and the Rutgers Research Council for financial support.

**Supplementary Material Available:** Tables of X-ray characterization data for **4** including listings of fractional coordinates, bond lengths, bond angles, thermal parameters, and hydrogen atom coordinates, spectroscopic and analytical data for **2–4**, and 1D and 2D NMR spectra for **3** (12 pages); listing of observed and calculated structure factors for **4** (12 pages). Ordering information is given on any current masthead page.

## Uranium(VI) Organoimido Complexes

Carol J. Burns,<sup>1a</sup> Wayne H. Smith,<sup>1b</sup> John C. Huffman,<sup>1c</sup> and Alfred P. Sattelberger\*,<sup>1a</sup>

*Inorganic and Structural Chemistry Group (INC-4) and  
Nuclear Materials Process Technology Group (NMT-2)  
Los Alamos National Laboratory  
Los Alamos, New Mexico 87545  
Molecular Structure Center, Indiana University  
Bloomington, Indiana 47405*

Received June 29, 1989

Complexes containing multiply bonded alkylidene, alkylidyne, imido, nitrido, and oxo ligands, and selected combinations thereof, are part of the tapestry of tungsten(VI) chemistry. There are numerous examples of such complexes, many of which were discovered within the past decade, and the interest in these high-energy systems stems, in large measure, from their ability to effect transformations of unsaturated organic and inorganic substrates.<sup>2</sup> The multiply bonded oxo group is well-known in discrete high-valent complexes of the next group 6 element, uranium, but nearly always in the form of the linear uranyl ion, UO<sub>2</sub><sup>2+</sup>.<sup>3</sup> Aside from uranyl complexes, the only reported molecular coordination compounds of U(VI) are UF<sub>6</sub>, UCl<sub>6</sub>, and the binary alkoxides, U(OR)<sub>6</sub>.<sup>3,4</sup> Uranium(VI) compounds containing

(1) (a) Inorganic and Structural Chemistry Group (INC-4), Mail Stop C346. (b) Nuclear Materials Process Technology Group (NMT-2), Mail Stop E501. (c) Molecular Structure Center, Indiana University.

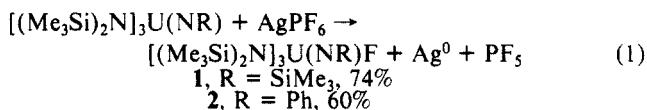
(2) Nugent, W. A.; Mayer, J. A. *Metal-Ligand Multiple Bonds*; Wiley: New York, 1988 and references therein.

(3) (a) Weigel, F. In *The Chemistry of the Actinide Elements*; Katz, J. J., Seaborg, G. T., Morss, L. R., Eds.; Chapman and Hall: New York, 1986; Chapter 5 and references therein. (b) Burns, C. J.; Sattelberger, A. P. *Inorg. Chem.* **1988**, 27, 3692. (c) Paine, R. T.; Ryan, R. R.; Asprey, L. B. *Inorg. Chem.* **1975**, 14, 1113. (d) Levy, J. H.; Taylor, J. C.; Wilson, P. W. *J. Inorg. Nucl. Chem.* **1977**, 39, 1989.

(4) Bachter, W.; Jacob, E. In *Handbook on the Physics and Chemistry of the Actinides*; Freeman, A. J., Keller, C., Eds.; Elsevier North-Holland: Amsterdam, 1985; Volume 3, Chapter 7 and references therein.

the other functional groups listed above have never been reported. Here we describe the synthesis and structural characterization of the first uranium(VI) systems containing a multiple bond to nitrogen.

The uranium(V) organoimido complexes  $[(\text{Me}_3\text{Si})_2\text{N}]_3\text{U}(\text{NSiMe}_3)^{5a,b}$  and  $[(\text{Me}_3\text{Si})_2\text{N}]_3\text{U}(\text{NPh})^{5b,c}$  were prepared by oxidation of  $\text{U}[\text{N}(\text{SiMe}_3)_2]_3^6$  with trimethylsilyl azide and phenyl azide, respectively. Cyclic voltammetry studies reveal that both complexes exhibit reversible one-electron oxidation waves at  $-0.41$  V ( $R = \text{SiMe}_3$ ) and  $-0.42$  V ( $R = \text{Ph}$ ) versus ferrocene as an internal standard.<sup>7</sup> These potentials lie in a convenient range for chemical oxidation by relatively mild reagents such as  $\text{Ag}^+$  or  $[(\text{C}_5\text{H}_5)_2\text{Fe}]^+$ . Reaction of the uranium(V) complexes with a suspension of  $\text{AgPF}_6$  in hexane for 6–8 h results in the formation of dark cherry red and red purple solutions for the silylimido and phenylimido compounds, respectively. Filtration to remove silver metal, concentration of the filtrates in vacuo, and slow cooling to  $-40^\circ\text{C}$  produces dark red prisms of the corresponding diamagnetic U(VI) organoimido fluoride complexes (eq 1).<sup>8</sup> Longer reaction times and/or a large excess of the silver reagent results in the formation of increasing amounts of a colorless byproduct, which has been identified as  $\{[(\text{Me}_3\text{Si})_2\text{N}]_4\text{Ag}\}_4$ . The properties of this complex will be reported elsewhere.<sup>9</sup>



The molecular structures of both uranium(VI) complexes have been determined by single-crystal X-ray diffraction.<sup>10</sup> ORTEP drawings are shown in Figure 1. Both complexes are trigonal bipyramidal with the bis(trimethylsilyl)amido groups occupying the equatorial positions. The F–U–N (imide) angles are near linear in both complexes ( $179.0(6)^\circ$  in 1,  $176.5(2)^\circ$  in 2), and the most significant deviation from idealized TBP geometry is a

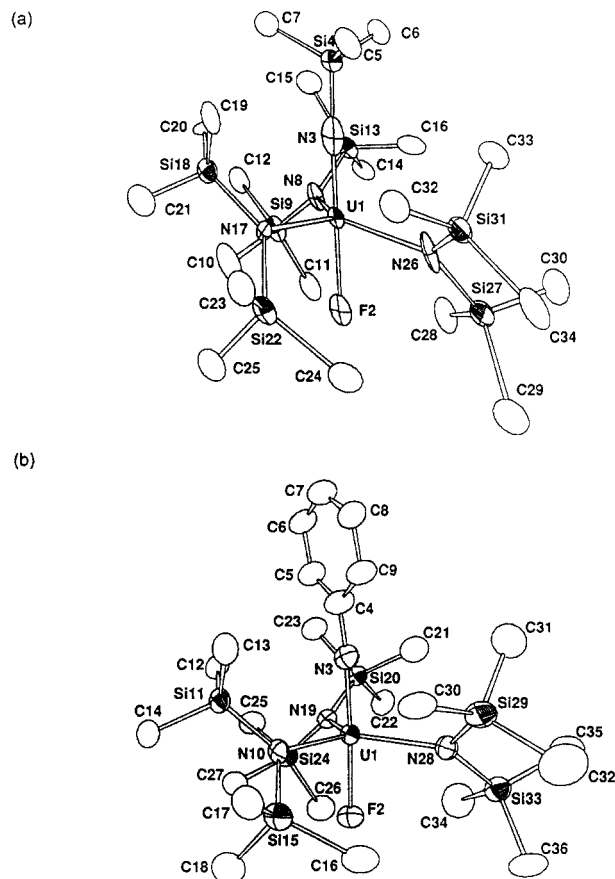


**Figure 1.** ORTEP drawings of (a)  $[(\text{Me}_3\text{Si})_2\text{N}]_3\text{U}(\text{NSiMe}_3)\text{F}$  and (b)  $[(\text{Me}_3\text{Si})_2\text{N}]_3\text{U}(\text{NPh})\text{F}$  with atom numbering schemes. Thermal ellipsoids are at the 30% probability level. Selected distances ( $\text{\AA}$ ) and angles ( $^\circ$ ) for 1:  $\text{U}(1)\text{--F}(2) = 2.013(12)$ ,  $\text{U}(1)\text{--N}(3) = 1.854(23)$ ,  $\text{U}(1)\text{--N}(8) = 2.252(17)$ ,  $\text{U}(1)\text{--N}(17) = 2.233(15)$ ,  $\text{U}(1)\text{--N}(26) = 2.217(17)$ ,  $\text{N}(3)\text{--U}(1)\text{--N}(8) = 94.8(7)$ ,  $\text{N}(3)\text{--U}(1)\text{--N}(17) = 94.4(7)$ ,  $\text{N}(3)\text{--U}(1)\text{--N}(26) = 94.1(8)$ ,  $\text{N}(8)\text{--U}(1)\text{--N}(17) = 117.6(6)$ ,  $\text{N}(8)\text{--U}(1)\text{--N}(26) = 120.7(6)$ ,  $\text{N}(17)\text{--U}(1)\text{--N}(26) = 120.0(6)$ . For 2:  $\text{U}(1)\text{--F}(2) = 2.068(5)$ ,  $\text{U}(1)\text{--N}(3) = 1.979(8)$ ,  $\text{U}(1)\text{--N}(10) = 2.206(7)$ ,  $\text{U}(1)\text{--N}(19) = 2.226(6)$ ,  $\text{U}(1)\text{--N}(28) = 2.219(6)$ ,  $\text{N}(3)\text{--U}(1)\text{--N}(10) = 90.1(3)$ ,  $\text{N}(3)\text{--U}(1)\text{--N}(19) = 95.4(3)$ ,  $\text{N}(3)\text{--U}(1)\text{--N}(28) = 92.2(3)$ ,  $\text{N}(10)\text{--U}(1)\text{--N}(19) = 117.9(2)$ ,  $\text{N}(10)\text{--U}(1)\text{--N}(28) = 120.2(3)$ ,  $\text{N}(19)\text{--U}(1)\text{--N}(28) = 121.3(2)$ .

slight bending of the amide groups out of the equatorial plane toward the fluoride ligand. The average F–U–N (amide) angle is  $85.6(5)^\circ$  in 1 and  $87.4(2)^\circ$  in 2. The U–N (amide) distance in the uranium(V) complex  $[(\text{Me}_3\text{Si})_2\text{N}]_3\text{U}(\text{NSiMe}_3)$  is  $2.295(10)$   $\text{\AA}$ .<sup>5a</sup> The average U–N (amide) bond length in compound 1 is  $2.234(16)$   $\text{\AA}$ , while that in 2 is  $2.217(6)$   $\text{\AA}$ . The large uncertainty in the bond lengths<sup>10a</sup> of 1, precludes quantitative discussion of the magnitude of the metal–ligand bond decrease upon oxidation, but the U–N (amide) bond lengths are shorter in the uranium(VI) imides, as would be expected from consideration of the smaller ionic radius of U(VI) relative to that of U(V).<sup>11</sup> We note that five-coordinate tungsten(VI) monoimido complexes have been reported, e.g.,  $(\text{NMe}_2)_4\text{W}(\text{NPh})^{12}$  and  $(\text{BZP})\text{W}(\text{N-}t\text{-Bu})(\text{HN-}t\text{-Bu})_2$  ( $\text{BZP} = \text{benzopinacolato dianion}$ ).<sup>13</sup> The former adopts a distorted square-pyramidal geometry, while the latter approximates a trigonal bipyramid with an axial imido group and equatorial amido ligands.

As in  $[(\text{Me}_3\text{Si})_2\text{N}]_3\text{U}(\text{NSiMe}_3)^{5a}$  and in the related cyclopentadienyl uranium imides,<sup>14–16</sup> the U–N–R angles in 1 and 2

(5) (a) Zalkin, A.; Brennan, J. G.; Andersen, R. A. *Acta Crystallogr.* **1988**, *C44*, 1553. (b) Brennan, J. G. Ph.D. Thesis, University of California—Berkeley, 1985. (c) Stewart, J. L. Ph.D. Thesis, University of California—Berkeley, 1988.

(6) Andersen, R. A. *Inorg. Chem.* **1979**, *18*, 1507.

(7) Cyclic voltammetry was conducted with a platinum working electrode and a silver wire quasi-reference electrode in a cell with anodic and cathodic compartments separated by a fine fritted glass disk. Tetra-*n*-butylammonium tetrafluoroborate (0.1 M in THF) was used as a supporting electrolyte, and the potential was swept at 200 mV/s.

(8)  $^1\text{H}$  NMR (250 MHz, toluene- $d_8$ ,  $25^\circ\text{C}$ ): 1,  $\delta$  0.76 (s, 27 H), 0.41 (s, 27 H), 0.12 (s, 9 H); 2,  $\delta$  0.85 (s, 27 H), 0.48 (s, 27 H), 9.06 (t, 2 H, meta), 2.03 (d, 2 H, ortho),  $-0.28$  (t, 1 H, para). IR (Nujol mull): 1, 1295 (vw), 1259 (m), 1246 (s), 1167 (vw), 1154 (vw), 926 (s), 882 (vs), 843 (vs), 769 (s), 757 (sh), 735 (w), 700 (w), 677 (w), 653 (s), 616 (s), 497 (w), 460 (vw)  $\text{cm}^{-1}$ ; 2, 3057 (w), 1583 (wbr), 1297 (vw), 1259 (m), 1248 (s), 1068 (vw), 1024 (vw), 932 (w), 903 (sh), 877 (vs), 846 (vs), 773 (s), 753 (m), 705 (w), 685 (m), 656 (s), 620 (s), 479 (m), 454 (w)  $\text{cm}^{-1}$ . MP: 1,  $136\text{--}138^\circ\text{C}$  dec; 2,  $112\text{--}115^\circ\text{C}$  dec. Combustion analytical data on both complexes were inconsistent. EI mass spectral data showed no molecular fragments higher than  $\text{HN}(\text{SiMe}_3)_2$ .

(9) Burns, C. J.; Sattelberger, A. P., manuscript in preparation.

(10) (a) 1: monoclinic space group  $P2_1/a$  with  $a = 18.458(15)$   $\text{\AA}$ ,  $b = 11.235(8)$   $\text{\AA}$ ,  $c = 18.035(16)$   $\text{\AA}$ ,  $\beta = 91.13(3)^\circ$ ,  $V = 3739(9)$   $\text{\AA}^3$ ,  $Z = 4$ , and  $d(\text{calc}) = 1.464$   $\text{g/cm}^3$ . Data were collected at  $-155^\circ\text{C}$  by utilizing Mo  $K\alpha$  radiation ( $\lambda = 0.71069$   $\text{\AA}$ ) and  $2\theta$  limits of  $6\text{--}45^\circ$ . Near the completion of the collection of data, the crystal fractured, and the resulting fragment diffracted at ca. 60% of the initial intensity. An overlapping (redundant) set of data was taken and a scaling factor determined prior to final data reduction. An absorption correction based on the initial measurement of the crystal led to higher disagreements between symmetrically equivalent data and was abandoned. The structure was solved by a combination of direct methods and Fourier techniques. Hydrogen atoms were placed in idealized positions; they were not refined. All non-hydrogen atoms were refined anisotropically. For 4040 reflections with  $F_o \geq 2.33\sigma(F_o)$ ,  $R = 0.0881$ ,  $R_w = 0.0822$ , GOF = 1.940. Despite repeated efforts, we have been unable to grow additional single crystals of 1 suitable for diffraction studies. (b) 2: monoclinic space group  $P2_1/c$  with  $a = 12.144(2)$   $\text{\AA}$ ,  $b = 30.402(9)$   $\text{\AA}$ ,  $c = 11.891(2)$   $\text{\AA}$ ,  $\beta = 121.60(1)^\circ$ ,  $V = 3739(3)$   $\text{\AA}^3$ ,  $Z = 4$ , and  $d(\text{calc}) = 1.473$   $\text{g/cm}^3$ . The data were collected at  $-155^\circ\text{C}$  by utilizing Mo  $K\alpha$  radiation ( $\lambda = 0.71069$   $\text{\AA}$ ) and  $2\theta$  limits of  $6\text{--}45^\circ$ . After application of an analytical absorption correction, the structure was solved by a combination of direct methods and Fourier techniques. All hydrogen atoms were located in a difference Fourier map and refined isotropically. All non-hydrogen atoms were refined anisotropically. For 4054 reflections with  $F_o \geq 2.33\sigma(F_o)$ ,  $R = 0.0421$ ,  $R_w = 0.0411$ , GOF = 1.214.

(11) Shannon, R. D. *Acta Crystallogr.* **1976**, *A32*, 751.

(12) Berg, D. M.; Sharp, P. R. *Inorg. Chem.* **1987**, *26*, 2959.

(13) Chan, D. M.-T.; Fultz, W. C.; Nugent, W. A.; Roe, D. C.; Tulip, T. H. *J. Am. Chem. Soc.* **1985**, *107*, 251.

(14) Brennan, J. G.; Andersen, R. A. *J. Am. Chem. Soc.* **1985**, *107*, 514.

(15) Cramer, R. E.; Panchanatheswaran, K.; Gilje, J. W. *J. Am. Chem. Soc.* **1984**, *106*, 1853.

are near linear (**1**, U(1)–N(3)–Si(4) = 178.3 (11)°; **2**, U(1)–N(3)–C(4) = 173.5 (7)°). In the case of (MeC<sub>3</sub>H<sub>4</sub>)<sub>3</sub>U(NPh), this linearity has been described as an indication of multiple bonding between uranium and nitrogen, with both lone pairs of the nitrogen being donated into e symmetry metal atomic orbitals to form a U≡N triple bond.<sup>14,16</sup> This bonding scheme also explains the unusually short uranium–imide nitrogen bond lengths. The latter range from 2.02 to 2.07 Å in the tris(cyclopentadienyl)uranium complexes,<sup>14–16</sup> while [(Me<sub>3</sub>Si)<sub>2</sub>N]<sub>3</sub>U(NSiMe<sub>3</sub>) displays a U–N (imide) bond length of 1.910 (16) Å.<sup>5a</sup> Oxidation to U(VI) should remove the final electron from a nonbonding f orbital, but one would expect a slight shortening of the U–N bond length due to the relative radii of U(V) and U(VI). The bond length U(1)–N(3) in complex **1** is 1.854 (23) Å, while in **2** this bond distance is 1.979 (8) Å. Within the error limits, there appears to be no significant difference in the metal–imide nitrogen bond lengths between the U(V) and U(VI) complexes. We believe this to be a reflection of the steric crowding about the metal center in the uranium(VI) systems. This crowding may also be the origin of the difference in U–N (imide) bond lengths between complexes **1** and **2**. The N(3)–Si(4) bond length (1.824 (24) Å) in **1** is substantially longer than the N(3)–C(4) bond length (1.392 (12) Å) in **2**. This decreases the steric demand of the imido ligand in **1**. The U–F bond lengths in **1** and **2** are 2.013 (12) and 2.068 (5) Å, respectively. For comparison, the mean U–F bond length in UF<sub>6</sub> is 1.995 (3) Å.<sup>17</sup>

Steric crowding about the uranium(VI) centers is also reflected in the solution behavior of the complexes. At room temperature, the <sup>1</sup>H NMR spectra of both monomers indicate a static structure, in which rotation about the equatorial U–N bonds is restricted, giving rise to inequivalent trimethylsilyl amide resonances. Upon warming, these resonances broaden and coalesce (60 °C for complex **1**, 55 °C for complex **2**). Continued heating results in the decomposition of the uranium(VI) complexes and the appearance of resonances due to *reduced* pyrolysis products. This solution decomposition also takes place over the course of several days at room temperature.

One unusual feature of the <sup>1</sup>H NMR spectrum of **2** is the location of the imido phenyl proton resonances at δ 9.06 (meta), 2.03 (ortho), and –0.28 (para). These resonances do not shift between –75 and +50 °C in toluene-*d*<sub>8</sub> and are observed at room temperature in THF-*d*<sub>8</sub>. We offer two possible explanations for this behavior: (1) a high degree of ionic character in the metal–imide nitrogen bond is resonance delocalized to the ortho and para carbons, which, in turn, shields the attached protons and shifts them to higher field, and/or (2) the uranium(VI) ion is a temperature-independent paramagnet (TIP). The latter behavior has been observed in several uranyl complexes.<sup>18–21</sup> Attempts to measure a (presumably) small TIP for solids **1** and **2** have been hampered by their thermal instability.

In summary, the first examples of uranium(VI) complexes with a multiple bond to a main-group element other than oxygen have been synthesized and structurally characterized. Whether uranium(VI) can be stabilized by multiply bonded ligands other than imido and oxo remains to be determined. We are presently operating under the assumption that, with the correct choice of ancillary ligands, uranium(VI) will support nitrido and perhaps even alkylidene and alkylidyne ligands in its coordination sphere.

**Acknowledgment.** We thank Dr. W. G. Van Der Sluys and Dr. D. L. Clark (LANL) for helpful discussions and Dr. M. W. McElfresh, IBM T. J. Watson Research Center, for his attempts

to measure the solid-state magnetic properties of **1** and **2**. C.J.B. is the recipient of a J. Robert Oppenheimer Fellowship at Los Alamos. The work was performed under the auspices of the Division of Chemical Sciences, Office of Energy Research, U.S. Department of Energy.

**Supplementary Material Available:** Tables of crystal data, atomic positional parameters, anisotropic thermal parameters, and selected bond lengths and angles for **1** and **2** (16 pages); tables of observed and calculated structure factors for **1** and **2** (22 pages). Ordering information is given on any current masthead page.

### Spontaneously Formed Functionally Active Avidin Monolayers on Metal Surfaces: A Strategy for Immobilizing Biological Reagents and Design of Piezoelectric Biosensors

Richard C. Ebersole, Jeffrey A. Miller, John R. Moran, and Michael D. Ward\*

Contribution No. 5382  
Central Research and Development Department  
E. I. du Pont de Nemours and Co., Experimental Station  
P.O. Box 80328, Wilmington, Delaware 19880-0328

Received December 20, 1989

Immobilization of biologically relevant entities for diagnostic assays<sup>1–4</sup> has been widely studied on polymeric and oxide supports. Immobilization on metallic surfaces, however, has not been investigated extensively. Such methodology is important for the design of electronic diagnostic sensors in which the transducing elements commonly include a metallic electrode, such as in electrochemical and piezoelectric devices. We report a novel strategy for immobilizing biological reagents on metallic surfaces and demonstrate its use in a DNA hybridization assay.

We find that robust, functionally active monolayers of avidin and streptavidin form spontaneously, and *irreversibly*, from aqueous solutions onto freshly evaporated gold and silver surfaces.<sup>5</sup> The ellipsometrically determined thicknesses were  $d(\text{avidin}) = 48$  Å and  $d(\text{streptavidin}) = 42$  Å, consistent with the presence of protein monolayers as inferred from the crystal structure of streptavidin.<sup>6</sup> The monolayers form rapidly (<10 min) under a wide range of conditions. Varying the NaCl concentration (0.1–1 M) or pH (3–11) had little effect on monolayer formation. The observation that both proteins form monolayers indicates that metal–sulfur interactions via cysteine residues are not a dominant factor, since cysteine is present in avidin but absent in streptavidin. The pI values for avidin and streptavidin are 10 and ca 7, respectively;<sup>7,8</sup> therefore, the absence of a pH effect indicates that

(1) Wilchek, M.; Bayer, E. A. *Anal. Biochem.* **1988**, *171*, 1–32.

(2) Henrikson, K. P.; Allen, S. H. G.; Maloy, W. L. *Anal. Biochem.* **1979**, *94*, 366–370.

(3) Gould, E. A.; Buckley, A.; Cammack, N. *J. Virol. Methods* **1985**, *11*, 41–48.

(4) Leary, J. J.; Brigati, D. J.; Ward, D. C. *Proc. Natl. Acad. Sci. U.S.A.* **1983**, *80*, 4045–4049.

(5) Gold and silver films (2000 Å) with chromium underlayers (200 Å) were prepared by evaporation at 25 Å s<sup>–1</sup> onto glass substrates or quartz crystals. Immediately upon removal from the evaporation chamber, the metal films were immersed in a phosphate buffered saline (PBS) solution (pH = 7.4) containing 0.2 mg/mL avidin or streptavidin (Sigma) for >10 min and then washed with PBS solution to remove unbound avidin. The monolayers could be stored either dry or in buffer solutions indefinitely at 4 °C without appreciable loss of activity. Monolayers prepared on aged metal films (>1 day) exhibited lower biotin binding activities.

(6) Weber, P. C.; Ohlendorf, D. H.; Wendoloski, J. J.; Salemme, F. R. *Science* **1989**, *243*, 85–88. Molecular modeling using the known structure of the streptavidin–biotin complex indicated approximate streptavidin molecular dimensions of 42 × 42 × 56 Å. The greater thickness observed for avidin is consistent with its larger molecular weight compared to streptavidin (the proteins avidin and streptavidin exist as tetramers with molecular weights of ≈67 000 and ≈60 000, respectively).

(16) Cramer, R. E.; Edelman, F.; Mori, A. L.; Roth, S.; Gilje, J. W.; Tatsumi, K.; Nakamura, A. *Organometallics* **1988**, *7*, 841.

(17) Levy, J. H.; Taylor, J. C.; Wilson, P. W. *J. Chem. Soc., Dalton Trans.* **1976**, 219.

(18) Eisenstein, J. C.; Pryce, M. H. L. *Proc. R. Soc. London, A* **1960**, *229*, 20.

(19) McGlynn, S. P.; Smith, J. K. *J. Mol. Spectrosc.* **1962**, *6*, 164.

(20) Denning, R. G.; Norris, J. O. W.; Short, I. G.; Snellgrove, T. R.; Woodmark, D. R. *ACS Symp. Ser.* **1980**, No. 131, 313.

(21) Denning, R. G.; Snellgrove, T. R.; Woodmark, D. R. *Mol. Phys.* **1979**, *37*, 1109.